Light with a twist : ray aspects in singular wave and quantum optics

Habraken, S.J.M.

4

Rotational stabilization and destabilization of an optical cavity

4.1 Introduction

Stability is a very distinctive property of the dynamics of a physical system. Characteristic for unstable dynamics is that an arbitrary initial state evolves into a rapidly diverging state. Examples range from the simple case of a particle on the top of a hill to a wealth of instabilities that can be observed and characterized in fluids and plasmas. External motion has significant effects on the dynamics of physical systems and may modify its stability properties. This is exemplified by the Paul trap [50], or more generally by a time-orbiting potential trap [51], in which a particle is trapped in an oscillating potential from which it would escape in the stationary case. The Paul trap is a close analogue of the rotational stabilization of a particle in a saddle-point potential [52]. Another well-known example of rotational stabilization is the gyroscope. Similar behavior has also been observed in thermodynamically large systems such as granular matter [53] and fluids [54].

In recent years, optical cavities with moving elements have become topical. State-of-the-art experiments focus on opto-mechanical oscillators driven by radiation pressure [55, 56] and cavity-assisted trapping and cooling [57, 58, 59]. Possible applications range from weak-force detection [60] to fundamental research on quantum entanglement [61, 62] and decoherence [63, 64] on macroscopic scales. In addition to the longitudinal radiation pressure, electromagnetic fields can exert transverse forces due to their phase structure [65]. A specific

example is the transfer of optical orbital angular momentum [21], which can give rise to a torque along the propagation axis of the beam. Recently, it has been shown that this torque can in principle be sufficiently large to trap and cool the rotational degrees of freedom of a mirror in a cavity-assisted set-up [25]. In this chapter, we focus on the complementary question: How does rotation of a mirror affect the optical properties of a cavity and, in particular, its (in)stability? As such, the work presented here constitutes the first analysis of rotational effects on stability in optics.

We consider a cavity that consists of two mirrors facing each other. In the standard case both mirrors are spherical. Depending on their focusing properties, a ray that is coupled into such a cavity can either be captured, or escape after a finite (and typically small) number of round trips. In the latter case the cavity is geometrically unstable whereas it is stable in the former one. The stability criterion for this system can be expressed as [12]

$$0 < g_1 g_2 < 1 \,, \tag{4.1}$$

where $g_{1,2} = 1 - L/R_{1,2}$ with $R_{1,2} = 2f_{1,2}$ the radii of curvature of the two mirrors, $f_{1,2}$ the corresponding focal lengths and L the mirror separation. The optical properties of unstable cavities are fundamentally different from those of their stable counterparts [12]. Since a geometrically stable cavity has the ability to confine light, its modes are spatially confined and stationary. An unstable cavity, on the other hand, cannot confine light and is intrinsically lossy even if the mirrors are perfectly reflecting. As a result, the propagation of light inside an unstable cavity is dominated by diffraction at the sharp edges of the mirrors [66] and its "modes" are self-similar diverging patterns that have a fractal nature [67]. Instability is a necessary condition for an optical cavity to display chaotic behavior [68].

We consider rotations about the optical axis of a cavity and expect an effect only if at least one of the mirrors is astigmatic (or cylindrical), so that the cavity lacks axial symmetry. In general, both mirrors can be astigmatic with non-parallel axes but, for simplicity, we first focus on a cavity that consists of a cylindrical (c) and a spherical (s) mirror. The more general case of a cavity with two astigmatic mirrors is briefly discussed in section 4.4. In the simple case of a cavity with one spherical and one astigmatic mirror, the curvature of each mirror can be specified by a single g parameter so that the configuration space, spanned by g_s and g_c, is two-dimensional. In the absence of rotation the stability criterion in the plane through the optical axis in which the cylindrical mirror is curved is of the form of equation (4.1): $0 < g_\mathrm{s} g_\mathrm{c} < 1$. In the other perpendicular plane through the cavity axis, in which the cylindrical mirror is flat, the stability criterion reads: $0 < g_\mathrm{s} < 1$. As is indicated in the stability diagram in the upper left window in figure 4.1, stable (dark blue) areas appear where both criteria are met. The cavity is partially stable (light blue) in areas where only one of the two is fulfilled. When a cavity is partially stable, both a ray that is coupled into it and its modes are confined in one of the two transverse directions only. One may guess that rotation disturbs the confinement of the light by the mirrors so that all (partially) stable cavities will eventually lose stability if the rotation frequency is sufficiently increased. However, we will show that this is not the case and that rotation has surprisingly rich and distinct effects on the

stability of a two-mirror cavity.

4.2 Stability of a rotating cavity

In order to describe the diffraction of light inside a rotating cavity, we use the paraxial approximation [45] and its generalization to the time-dependent case [46]. We write the transverse electric field of a propagating mode as

$$\mathbf{E}(\mathbf{r},t) = \mathrm{Re}\left\{E_0 \epsilon u(\mathbf{r},t) e^{ikz-i\omega t}\right\} , \tag{4.2}$$

where E_0 is the amplitude of the field, ϵ is the polarization, k is the wave number and $\omega = ck$ is the optical frequency with c the speed of light. The large-scale spatial structure and slow temporal variations of the electric field are characterized by the complex scalar profile $u(\mathbf{r},t)$. In lowest order of the paraxial approximation and under the assumption that the time dependence of the profile is slow compared to the optical time scale, the electric field is purely transverse and the profile $u(\mathbf{r},t)$ obeys the time-dependent paraxial wave equation

$$\left(\nabla_\rho^2 + 2ik\frac{\partial}{\partial z} + \frac{2ik}{c}\frac{\partial}{\partial t}\right) u(\mathbf{r},t) = 0 , \tag{4.3}$$

with $\nabla_\rho^2 = \partial^2/\partial x^2 + \partial^2/\partial y^2$. If we omit the derivative with respect to time, this equation reduces to the standard paraxial wave equation, which describes the diffraction of a freely propagating stationary paraxial beam. The additional time derivative accounts for the time dependence of the profile and incorporates retardation between distant transverse planes.

The dynamics of light inside a cavity is governed by the boundary condition that the electric field vanish on the mirror surfaces. For a rotating cavity, this boundary condition is explicitly time dependent. This homogeneous time dependence vanishes in a co-rotating frame where it is sufficient to consider time-independent propagating modes $v(\mathbf{r})$. The transformation that connects $v(\mathbf{r})$ and $u(\mathbf{r},t)$ takes the form

$$u(\mathbf{r},t) = \hat{U}_{\mathrm{rot}}(\Omega t) v(\mathbf{r}) , \tag{4.4}$$

where Ω is the rotation frequency and $\hat{U}_{\mathrm{rot}}(\alpha) = \exp(-i\alpha\hat{L}_z)$ is the operator that rotates a scalar function over an angle α about the z axis with $\hat{L}_z = -i(x\partial/\partial y - y\partial/\partial x)$ the z component of the orbital angular momentum operator. Substitution of the rotating mode (4.4) in the time-dependent wave equation (4.3) gives

$$\left(\nabla_\rho^2 + 2ik\frac{\partial}{\partial z} + \frac{2\Omega k}{c}\hat{L}_z\right) v(\mathbf{r}) = 0 \tag{4.5}$$

for $v(\mathbf{r})$. The transformation to a rotating frame gives rise to a Coriolis term, in analogy with particle mechanics. Since ∇_ρ^2 and $\hat{L}_z$ commute, the formal solution of equation (4.5) can be expressed as

$$v(\rho,z) = \hat{U}_{\mathrm{f}}(z)\hat{U}_{\mathrm{rot}}\left(-\frac{\Omega z}{c}\right) v(\rho,0) \equiv \hat{U}(z) v(\rho,0) , \tag{4.6}$$

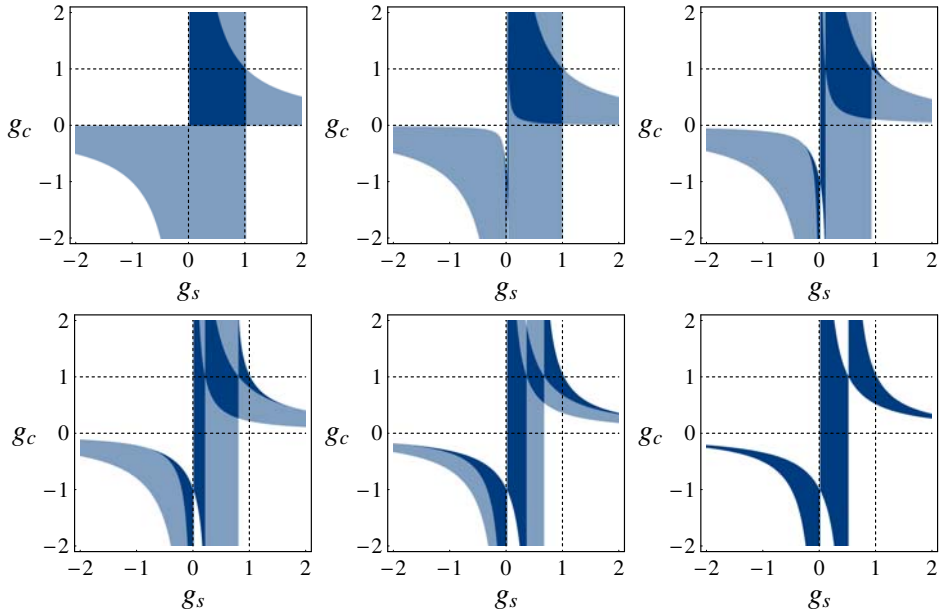

Figure 4.1: Stable (dark blue), partially stable (light blue) and unstable (white) areas of the configuration space (g_s, g_c) for a cavity that consists of a stationary spherical and a rotating cylindrical mirror, for different rotation frequencies. From left to right and from top to bottom the rotation frequency is increased in equal steps $\Omega_0/20$ from 0 to $\Omega_0/4$.

where $\rho = (x, y)^{\mathrm{T}}$ and $\hat{U}_{\mathrm{f}}(z) = \exp\left(\frac{iz}{2k}\nabla_\rho^2\right)$ is the unitary operator that describes free propagation of a paraxial beam in a stationary frame. The operator $\hat{U}(z)$ has the significance of the propagator in the rotating frame. The rotation operator arises from the Coriolis term in equation (4.5) and gives the propagating modes a twisted nature.

The transformation of paraxial modes under propagation and optical elements can be expressed in terms of a ray ($ABCD$) matrix [12, 32]. The standard 2×2 ray matrices that describe optical elements with axial symmetry can be found in any textbook on optics. The ray matrix of a composite system can be constructed by multiplying the ray matrices that describe the optical elements and the distances of free propagation between them, in the proper order. Generalization to astigmatic optical elements is straightforward and requires 4×4 ray matrices [12]. The ray matrix that describes propagation in a rotating frame is, analogous to equation (4.6), given by $M(z) = M_{\mathrm{f}}(z)M_{\mathrm{rot}}(-\Omega z/c)$, where $M_{\mathrm{f}}(z)$ is the 4×4 ray matrix that describes free propagation over a distance z and $M_{\mathrm{rot}}(\alpha)$ is the 4×4 ray matrix that rotates the position ρ and propagation direction θ of a ray $\mathscr{z}^{\mathrm{T}} = (\rho^{\mathrm{T}}, \theta^{\mathrm{T}})$ over an angle α about the z axis. Starting at the entrance plane of the spherical mirror, the time-independent ray matrix that describes a round trip through the rotating cavity in the co-rotating frame is

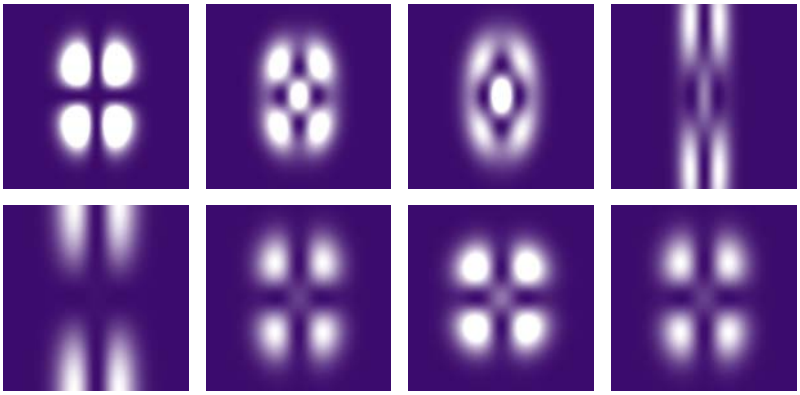

Figure 4.2: Transverse intensity patterns in the co-rotating frame of the $(1, 1)$ mode of cavity I (top), which is specified by $(g_s, g_c) = (\frac{3}{4}, \frac{1}{2})$ and destabilized by rotation, and cavity II (bottom), which is specified by $(g_s, g_c) = (-\frac{3}{4}, -\frac{1}{2})$ and stabilized by rotation, for increasing rotation frequencies. From left to right it increases from 0 to $0.166\Omega_0$ for cavity I and from $0.21\Omega_0$ to $\Omega_0/4$ for cavity II. The plots show the mode patterns close to the spherical mirror and the vertical direction corresponds to the direction in which the cylindrical mirror is flat.

then

$$M_{\mathrm{rt}} = M(L) \cdot M_{\mathrm{c}} \cdot M(L) \cdot M_{\mathrm{s}} \,, \tag{4.7}$$

where L is the mirror separation and M_{s} and M_{c} are the ray matrices for the spherical and the cylindrical mirror. They are fully determined by the radii of curvature and the orientation of the mirrors in the transverse plane. Explicit expressions of these ray matrices are given in sections 2.2 and 3.5.

Typically, the round-trip ray matrix (4.7) has four distinct time-independent eigenvectors μ_i with corresponding eigenvalues λ_i. In the rotating frame, any time-dependent incident ray $\mathscr{r}_0^{\mathrm{T}}(t) = \left(\rho^{\mathrm{T}}(t), \theta^{\mathrm{T}}(t)\right)$ can be expanded as $\mathscr{r}_0(t) = \sum_i a_i(t)\mu_i$. After n times bouncing back and forth between the mirrors, the ray evolves into $\mathscr{r}_n(t + 2nL/c) = \sum_i a_i(t)\lambda_i^n\mu_i$. The possibly complex eigenvalues have the significance of the magnification of the eigenvector after one round trip and it follows that a cavity is stable only if all four eigenvalues have absolute value 1. As shown in chapter 2, the eigenvalues of any physical ray matrix come in pairs λ and λ^{-1} so that possible deviations from $|\lambda| = 1$ appear in two of the four eigenvalues at the same time. If only two eigenvalues have absolute value 1, the cavity is partially stable. The eigenvalues of the round-trip ray matrix (4.7) do not depend on the frame of reference, and it follows that the same is true for the notion of stability.

A ray that is bounced back and forth inside the cavity hits a mirror at time intervals L/c. Since a rotation over π turns an astigmatic mirror to an equivalent orientation, it follows that the stability of a cavity is not affected by a change in the rotation frequency $\Omega \to \Omega + p\Omega_0$

with integer p and $\Omega_0 = c\pi/L$. In the present case, in which one of the mirrors is spherical, a ray hits the cylindrical mirror at time intervals $2L/c$ so that the eigenvalues λ_i are periodic with $\Omega_0/2$. Moreover, an astigmatic cavity is not gyrotropic so that the eigenvalues do not depend on the sign of Ω. It follows that it is sufficient to only consider rotation frequencies in the range $0 < \Omega < \Omega_0/4$.

By using the expression of the ray matrix in the co-rotating frame (4.7) and the stability criterion that its eigenvalues must have a unit length, we find the stable, partially stable and unstable sections in the configuration space $(g_\mathrm{s}, g_\mathrm{c})$ for different values of the rotation frequency. The results are shown in figure 4.1. These plots reveal that, already at relatively small rotation frequencies, quite drastic changes take place. For instance, near $(g_\mathrm{s}, g_\mathrm{c}) = (1, 0)$ stable configurations are destabilized to become (partially) unstable, while partially stable geometries near the negative g_c axis are stabilized by the rotation. An optical cavity can thus both lose and gain the ability to confine light due to the fact that it rotates. It is noteworthy that some configurations, for example those with small and positive g_s and g_c, are first partially destabilized by rotation, but retrieve stability if the rotation frequency is further increased. Another remarkable feature of the plots in figure 4.1 is the absence of partially stable areas in the lower right plot. As we will argue below, this is more generally true for the rotation frequency $\Omega_0/4$. In this specific case, the boundaries of stability are given by the hyperbolas $g_c = 1/(2g_s)$ and $g_c = 1/(2g_s - 1)$ and their asymptotes.

4.3 Signatures of stabilization and destabilization

As discussed in chapter 3, the structure of the modes of a rotating cavity is fully determined by the eigenvectors μ_i. The modes are defined as co-rotating solutions of the time-dependent paraxial wave equation (4.3) that vanish on the mirror surfaces. Geometric stability comes in as the necessary and sufficient requirement for them to exist. Here, we illustrate the effect of rotational (de)stabilization on the mode structure by considering two cases of a cavity with a spherical and a cylindrical mirror. Cavity I is specified by $(g_\mathrm{s}, g_\mathrm{c}) = (\frac{3}{4}, \frac{1}{2})$. It is stable in the absence of rotation and destabilized at a rotation frequency $\Omega = \Omega_0/6$. Cavity II is specified by the parameter values $(g_\mathrm{s}, g_\mathrm{c}) = (-\frac{3}{4}, -\frac{1}{2})$. It is partially stable in the absence of rotation and stabilized by rotation at $\Omega \simeq 0.2098\Omega_0$. The effect of rotation on the spatial structure of the modes of cavities I and II is shown in figure 4.2. The upper frames show the transverse spatial structure on the spherical mirror of the $(1, 1)$ mode of cavity I. From left to right the rotation frequency increases from 0 to $0.166\Omega_0$ in equal steps. In the absence of rotation (left frame) the mode is an astigmatic Hermite-Gaussian mode. Due to rotation, the mode is deformed to a generalized Gaussian mode with a nature in between Hermite-Gaussian and Laguerre-Gaussian modes [44]. As a result, phase singularities or so-called optical vortices [14], which are visible as points with zero intensity, appear. For rotation frequencies close to $\Omega_0/6$, the mode loses its confinement in the vertical direction. This reflects the fact that the cavity approaches a region of partial instability. The lower frames in figure 4.2 show the intensity pattern on the spherical mirror of the $(1, 1)$ mode of cavity II, which is stabilized

by rotation. From left to right the rotation frequency is increased from $0.21\Omega_0$ to $0.25\Omega_0$ in equal steps. As a result of the rotation we retrieve a mode that is confined in both directions and is similar to a Hermite-Gaussian mode. Deformation of the mode due to the rotation is more pronounced for even larger values of the rotation frequency.

Obviously, the horizontal and vertical directions in figure 4.2, which correspond to the curved and flat directions of the cylindrical mirror, are lines of symmetry. In the special case of a rotation frequency $\Omega_0/4$, the cylindrical mirror is rotated over $\pi/2$ after each round trip so that its orientation is periodic with two round-trip times as a period. This causes the diagonal lines between the horizontal and vertical directions to be lines of symmetry of the round-trip ray matrix (4.7) and the intensity patterns. This explains the apparent absence of astigmatism in the lower right plot of figure 4.2. This additional symmetry also causes the four eigenvalues λ_i to have the same absolute value, which explains the absence of partial stability in the lower right plot of figure 4.1.

Although the intensity patterns of the modes are aligned along the axes of the cylindrical mirror, their phase patterns are not. These attain a twist that is a signature of orbital angular momentum [21, 17], proportional to $\int d\rho v^*(\rho, z)\hat{L}_z v(\rho, z)$. The dependence of this orbital angular momentum in the $(1, 1)$ mode of cavity I on the rotation frequency is shown in figure 4.3 (left plot). The orbital angular momentum shows a divergence at $\Omega_0/6$, which arises from the induced instability of the cavity. The opposite happens for cavity II (right plot), which is stabilized by rotation. In this case the orbital angular momentum decreases with increasing rotation frequencies and eventually vanishes for $\Omega = \Omega_0/4$ due to the additional symmetry at this specific rotation frequency. The vanishing orbital angular momentum does not imply that there is no vorticity in the modes at this rotation frequency. The two contributions to the orbital angular momentum add up to zero for modes with two equal mode numbers.

4.4 Two astigmatic mirrors

Some features of the set-up that we have discussed so far are specific for the relatively simple geometry we have looked at. In particular, the plots in figure 4.1 show that no cavity with one spherical and one cylindrical mirror that is unstable in the absence of rotation can be (partially) stabilized by rotation. This is different in more general cases. As an example, we consider a cavity with two astigmatic mirrors. We take one of the radii of curvature of each of the mirrors fixed while we vary the others. In this case the corresponding parameter space, spanned by the g parameters corresponding to the varying radii of curvature, is again two-dimensional. The radii of curvature are chosen such that the g parameters are given by $(3/4, g_1)$ for mirror 1 and $(g_2, 3/4)$ for mirror 2. The alignment of the mirrors is such that the g_1 direction of mirror 1 is parallel to the $3/4$ direction of mirror 2 (and vice versa) so that the cavity has simple astigmatism. In the absence of rotation each of the symmetry planes through the mirror axes and the cavity axis can be considered as a cavity with two spherical mirrors. The corresponding stability criteria are given by $0 < 3g_1/4 < 1$ for one symmetry plane and $0 < 3g_2/4 < 1$ for the other. As is indicated in the upper left window in figure 4.4,

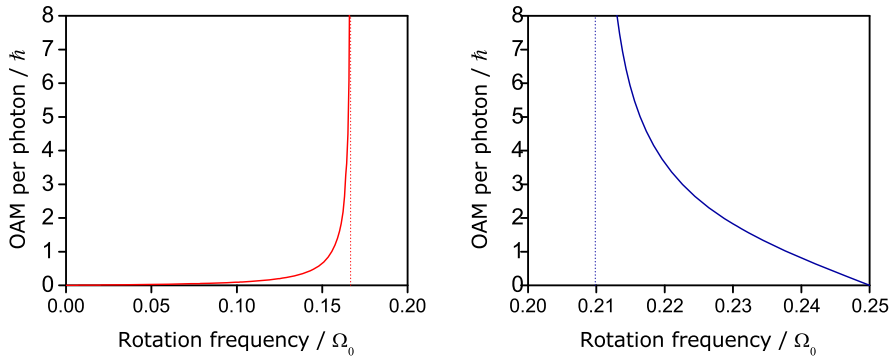

Figure 4.3: Dependence on the rotation frequency of the orbital angular momentum per photon in the $(1, 1)$ mode of cavity I (left), which is destabilized by rotation, and cavity II (right), which is stabilized by rotation.

these criteria are met in strips in the configuration space (g_1, g_2). A cavity with two astigmatic mirrors lacks the additional symmetry at $\Omega_0/4$ so that we need to consider rotation frequencies in the range $0 < \Omega < \Omega_0/2$. As the other windows in figure 4.4 reveal, again rotation has profound effects on the (in)stability of the cavity. One of the striking differences with the plots in figure 4.1 is that some unstable geometries, in particular close to $(g_1, g_2) = (1, 1)$ are fully stabilized by rotation at relatively small values of the rotation frequency. At the specific value of the rotation frequency $\Omega_0/2$, the mirrors are rotated over $\pi/2$ while the light propagates from one mirror to the other. From the stability point of view, this situation is equivalent to the case in which the mirrors are in the anti-parallel alignment and non-rotating. In that case, the stability criteria can be expressed as $0 < g_1 g_2 < 1$, which gives rise to hyperbolic boundaries of stability, and $0 < 9/16 < 1$, which is always fulfilled. As a result the cavity is partially stable in all cases and fully stable between the hyperbola $g_1 = 1/g_2$ and the $g_1 = 0$ and $g_2 = 0$ axes in the configuration space. This is confirmed by the stability diagram in the lower right window in figure 4.4. As a result of the fact that all geometries are (at least) partially stable at the rotation frequency $\Omega_0/2$, there is a strange discontinuity in the stability diagrams. Here, it occurs at $\Omega \simeq 0.27\Omega_0$. At this value of the rotation frequency many unstable geometries are suddenly partially stabilized while stable geometries are fully destabilized. Partially stable configurations are both stabilized to become stable and destabilized to become unstable. However, no configurations are stable through this sharp transition, which, physically speaking, corresponds to the boundary between "similar to anti-parallel alignment" and "similar to parallel alignment" of the mirrors.

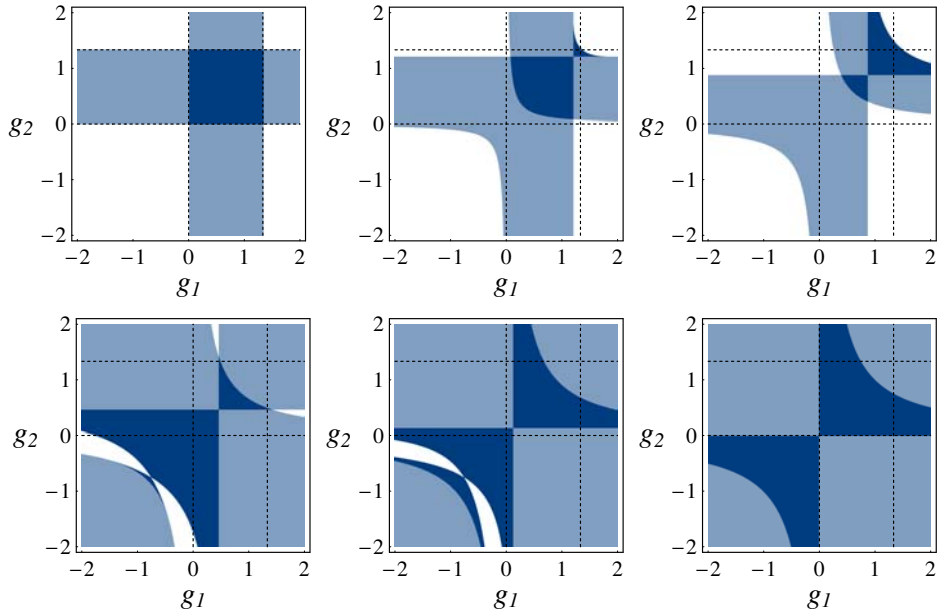

Figure 4.4: Stable (dark blue), partially stable (light blue) and unstable (white) areas of the configuration space (g_1, g_2) for a cavity that consists of two astigmatic mirrors, for different rotation frequencies. The g parameters corresponding to the radii of curvature of mirror 1 are given by $(3/4, g_1)$ while the g parameters for mirror 2 are given by $(g_2, 3/4)$. From left to right and from top to bottom the rotation frequency is increased in equal steps $\Omega_0/20$ from 0 to $\Omega_0/4$.

4.5 Conclusion

We have investigated rotationally induced transitions between the areas of stability and partial instability of an astigmatic two-mirror cavity. This is the first example of an optical system where stability can be induced or removed by rotation. Mechanical systems with dynamical stabilization are the Paul trap and the gyroscope. The most obvious signatures of rotational (de)stabilization are the modification of the mode confinement and the divergence of the orbital angular momentum, discussed in section 4.3 and respectively shown in figures 4.2 and 4.3. The spatial structure of the rotating cavity modes may be difficult to measure, but since their orbital angular momentum components appear at different frequencies due to the rotational Doppler shift [48, 69], it should be possible to resolve the divergence of the orbital angular momentum spectroscopically. The effects of transverse rotations on the optical properties of a cavity are significantly more complex than the resonance shifts that are associated with small longitudinal displacements of the mirrors. This may have important consequences in cavity-assisted opto-mechanical experiments in which the rotational degrees of freedom of

a mirror are addressed.

Although the set-up that we have studied here is rather specific, our method, which is exact in the paraxial limit, can be applied to more complex optical systems. Moreover, it should also be applicable to other, mathematically similar, wave-mechanical systems. Examples include the quantum-mechanical description of a particle in a rotating, partially stable potential and rotating acoustical cavities. In particular, the modification of the mode confinement and the rotationally induced angular momentum are expected to have analogues in such systems.